

CRISPR transcriptional repression devices and layered circuits in mammalian cells

Samira Kiani^{1,2}, Jacob Beal³, Mohammad R Ebrahimkhani², Jin Huh^{1,2,4}, Richard N. Hall^{1,2},
Zhen Xie⁵, Yingqing Li⁶, Ron Weiss^{1,2,6}

¹Synthetic Biology Center, Massachusetts Institute of Technology, Cambridge, MA 02139, USA

²Department of Biological Engineering, Massachusetts Institute of Technology, Cambridge, MA 02139, USA

³ Raytheon BBN Technologies, Cambridge, MA, 02138, USA

⁴Institute for the BioCentury, Korea Advanced Institute of Science and Technology, Daejeon, South Korea

⁵Bioinformatics Division/Center for Synthetic & Systems Biology, Tsinghua National Laboratory for Information Science and Technology; Department of Automation, Tsinghua University, Beijing, 100084, China

⁶ Department of Electrical Engineering and Computer Science, Massachusetts Institute of Technology, Cambridge, MA 02142, USA

Address correspondence to: Ron Weiss, Massachusetts Institute of Technology (MIT)
Synthetic Biology Center,
Building NE47,
500 Technology Square
Cambridge, MA 02139, USA. Tel: +1 617 253 8966; Fax: +1 617 452 2631; Email:
rweiss@mit.edu

Contents

Supplementary figure 1 Model of CRISPR based repression device performance.

Supplementary Figure 2 CR-U6 design and optimization.

Supplementary Figure 3 CRISPR Repression device based on standard *U6* promoter in human cells.

Supplementary Figure 4 Analysis of cross-talk between gRNAs and *CRP-a* or *CRP-b* promoters.

Supplementary figure 5 Output EYFP as a function of constitutive fluorescent protein for *U6/CRa-U6/CRP-b* cascade.

Supplementary Figure 6 Design and function of direct gRNA-a regulation by *TRE* promoter, an RNA Pol II promoter.

Supplementary Figure 7 Design and function of intronic gRNA (igRNA) based repression device.

Supplementary Figure 8 Investigating the reversibility of inducible CRISPR transcriptional repression devices.

Supplementary Figure 9 Repression of output in the intronic gRNA device is not due to overexpression of mKate protein and load on host cellular resources.

Supplementary Figure 10 Cas9m and igRNA-a repression is reduced by modification of intronic branch point sequence.

Supplementary Figure 11 igRNA device library showing the nucleotide sequence of target sites at *CRP* promoters and corresponding guide sequence on igRNA.

Supplementary Figure 12 Cascade circuit based on layering U6 driven gRNA-a and CRP driven igRNA-b.

Supplementary Figure 13 Cascade circuit based on layering U6 driven gRNA-b and CRP-b/igRNA-a.

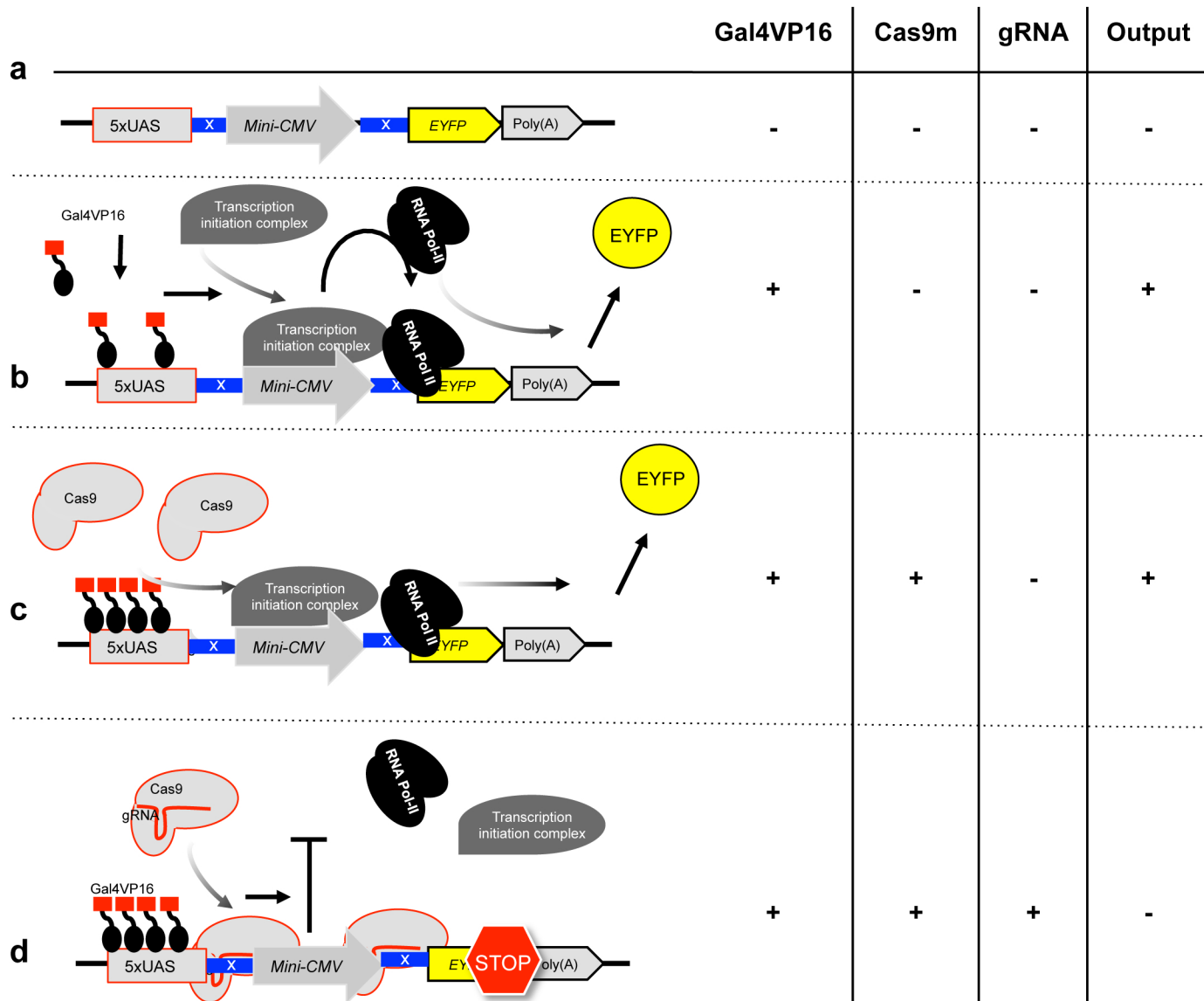
Supplementary Figure 14 Three cascades of transcriptional repression devices with stage 1 gRNAs expressed from RNA Pol II promoters.

Supplementary Figure 15 Typical distribution of constitutive fluorescence

Supplementary Discussion

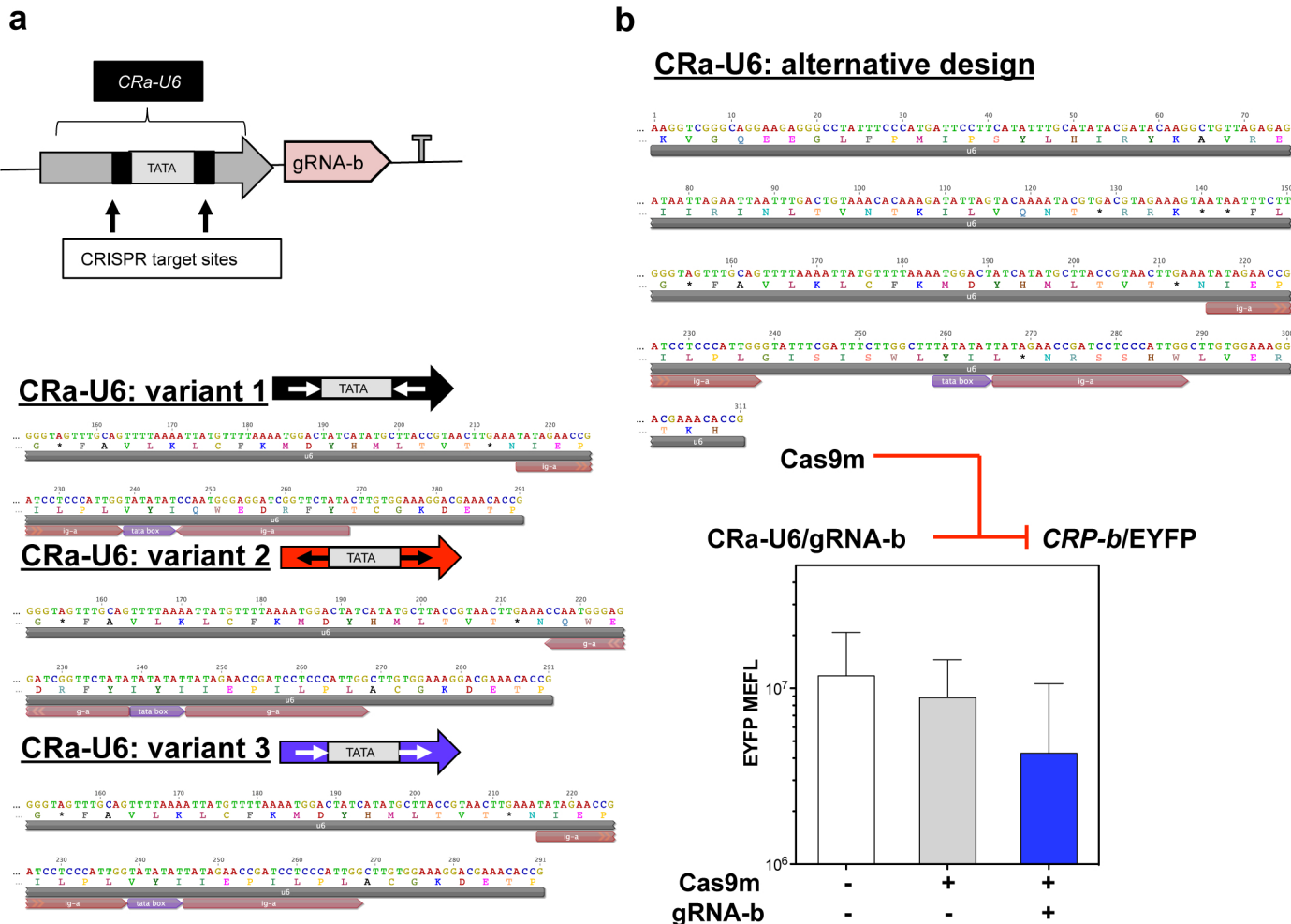
Supplementary Notes

Supplementary figure 1 Model of CRISPR based repression device performance.



Proposed mechanism of CRISPR-based transcriptional repression devices. (a) We designed the CRISPR responsive promoter (CRP) architecture based on Cas9m-mediated steric blocking of transcription. The CRP core region is the well-understood and widely used *mini-CMV* promoter, which the pre-initiation complex binds. Upstream UAS sites for Gal4 binding enable up-regulation by the Gal4VP16 activator. Flanking the *mini-CMV* promoter are two Cas9 target sites that enable Cas9m/gRNA mediated transcriptional repression of downstream genes by steric hindrance of assembly of the initiation complex. In the absence of Gal4VP16, the initiation complex does not bind the *mini-CMV* promoter and the downstream gene, *EYFP*, is not transcribed. (b) In the presence of Gal4VP16, which recruits transcription initiation complex, RNA polymerase II is able to assemble and initiate transcription. (c) In the presence of Cas9m but not gRNA complementary to sequences flanking the *mini-CMV* promoter, Cas9m does not bind DNA and transcription of downstream gene remains active. (d) In the presence of both Cas9m and gRNA, the complex binds the complementary regions flanking *mini-CMV* promoter and sterically blocks pre-initiation complex assembly, hence, inhibiting transcription initiation. This proposed model does not rule out other possible mechanisms that may be involved in the observed CRISPR mediated repression effect.

Supplementary Figure 2 CR-U6 design and optimization.



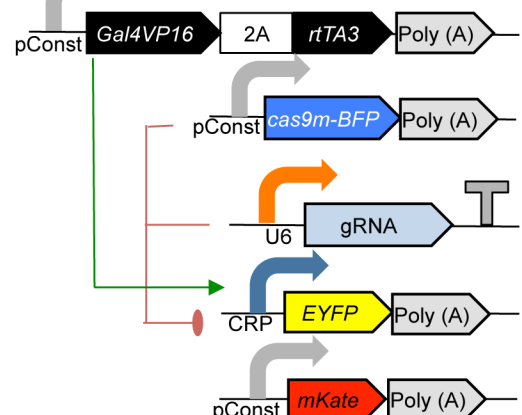
(a) CRa-U6/gRNA-b design. Two gRNA-a target sites are inserted within the *U6* promoter flanking TATA sequence. Different variants refer to directionality of gRNA-a target sites flanking TATA sequence in *U6* promoter. In variant 1, upstream target site is located at sense strand (positive) and the downstream one is inserted in the antisense (negative) strand. Variant 2 is negative-positive with respect to the directionality of upstream and downstream target sites. Variant 3 is positive-positive with respect to the directionality of upstream and downstream target sites. **(b)** Alternative design of CR-U6 : Two gRNA-a binding sites are inserted within the *U6* promoters flanking the TATA sequence with about 20bp space between the upstream target sites and TATA sequence. This modification appears to significantly diminish baseline promoter strength as analyzed in a transcriptional repression circuit that tests expression of gRNA from CR-U6 and regulation of EYFP production by CRP similar to circuit in Fig. 1a. HEK293 cells were transfected with empty plasmids, Cas9m or Cas9m and gRNA-b encoded from CRa-U6 promoter and EYFP was measured by flow cytometry 48 hours post transfection. Bars show geometric mean and standard deviation of mean of EYFP MEFL for cells expressing $\geq 10^6$ MEFL transfection marker mKate. $n=4$ biological replicates pooled from three representative experiments.

Supplementary figure 3 CRISPR Repression device based on standard *U6* prompter in human cells.

a

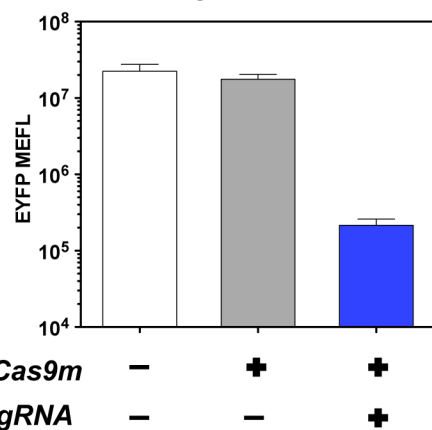
input gRNA	Target sequence at hybrid promoter
gRNA-a	TATAGAACCGATCCTCCCATTGG
gRNA-b	TACCTCATCAGGAACATGTTGG

b



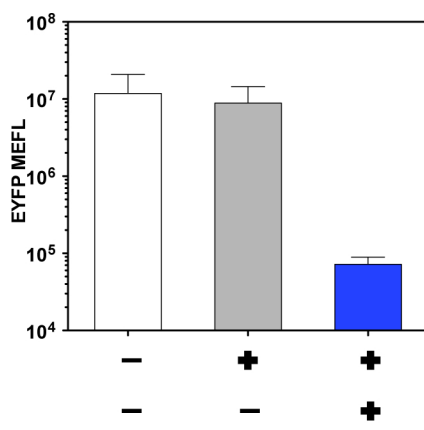
c

gRNA-a

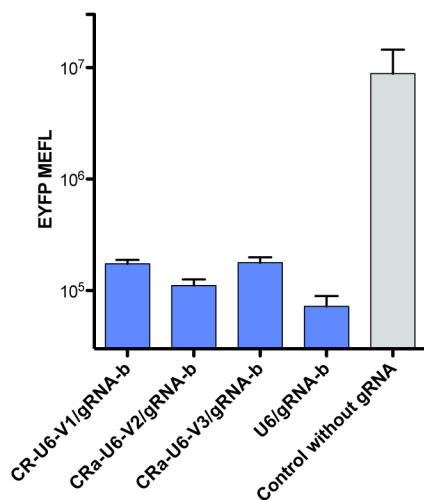


d

gRNA-b

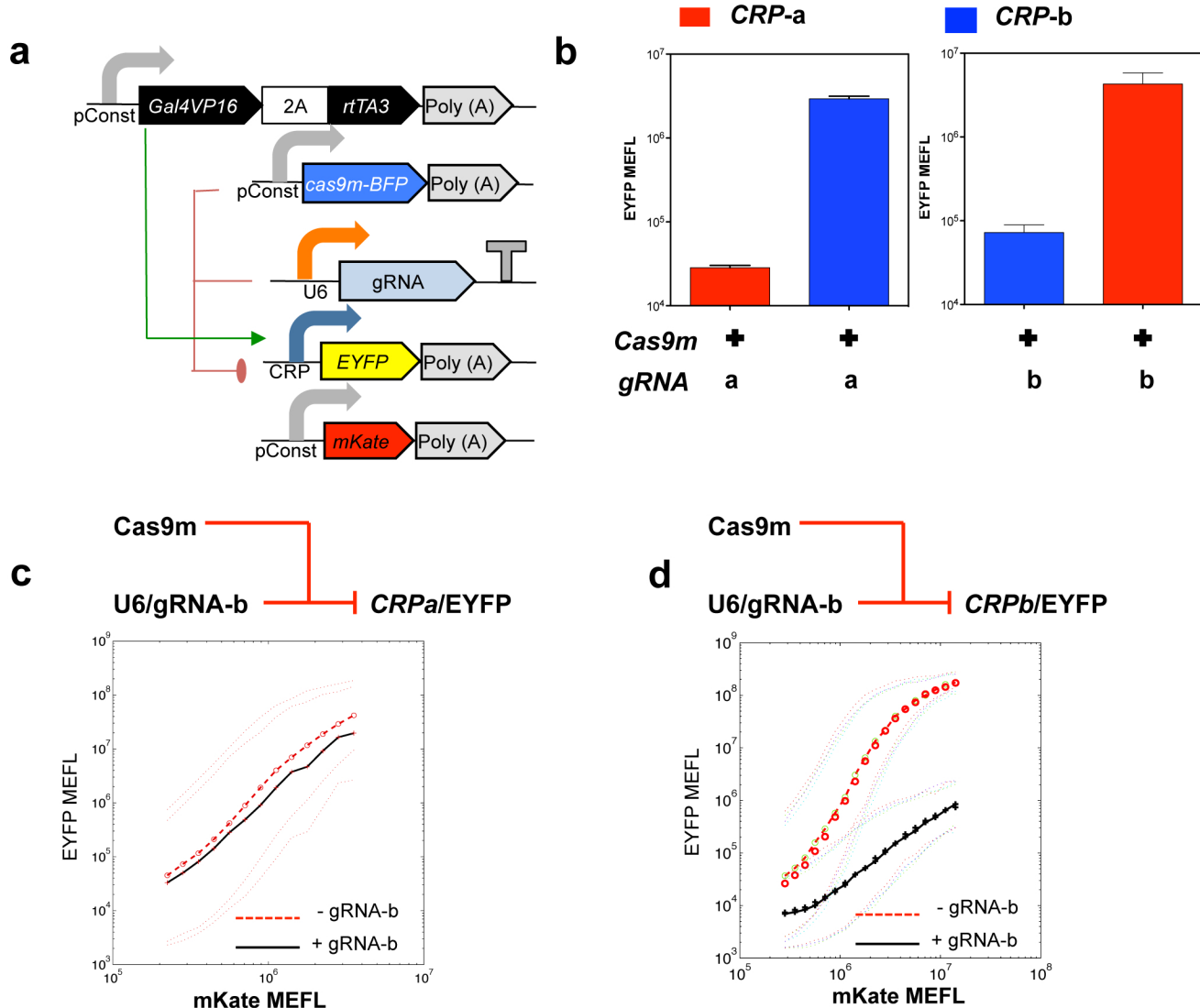


e



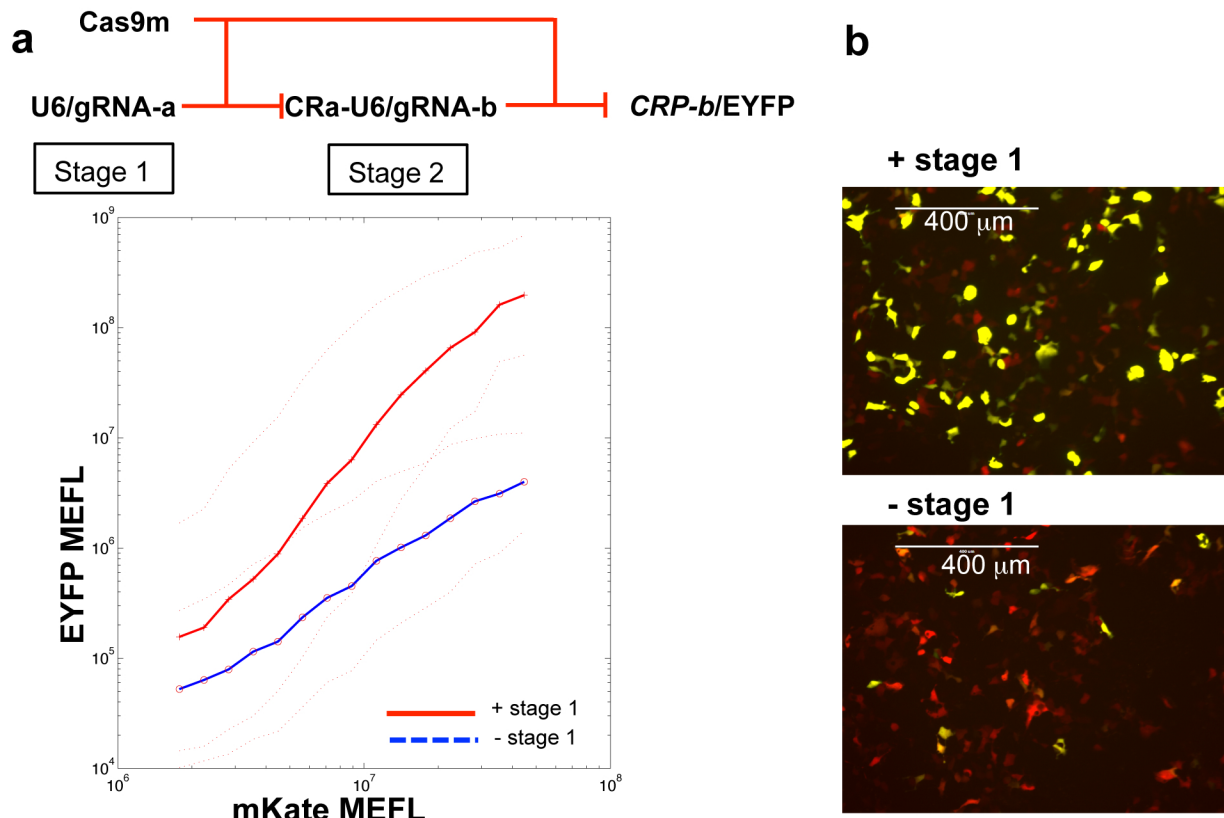
(a) gRNA target sites in *CRP-a* and *CRP-b*. **(b)** Characterization of *CRP* repression device with gRNA expressed from unmodified *U6* promoter: EYFP expression is activated by Gal4VP16 that binds cognate sites at the *CRP* promoter and is repressed by *U6* driven gRNA mediated targeting of Cas9m to CRPs. mKate fluorescent protein serves as the transfection marker. **(c-d)** EYFP output fluorescence for circuits in panel b for samples transfected with or without Cas9m and *U6*- driven gRNA-a or b. Bar graphs are geometric mean and standard deviation of EYFP MEFL means for cells expressing > 10⁶ MEFL of transfection marker mKate. *n*=3 biological replicates from one of two representative experiments. **(e)** Side by side comparison of RNA Pol III driven gRNA-b devices presented throughout this study. All data have been reported in other figures. Bar graph represents geometric mean and standard deviation of EYFP mean in samples transfected with all units of devices (gRNA and Cas9). Gray bar represents the control group in the absence of gRNA unit and presence of all other units. Please note that the CR-U6 devices have comparable efficiency to standard *U6*.

Supplementary Figure 4 Analysis of cross-talk between gRNAs and CRP-a or CRP-b promoters.



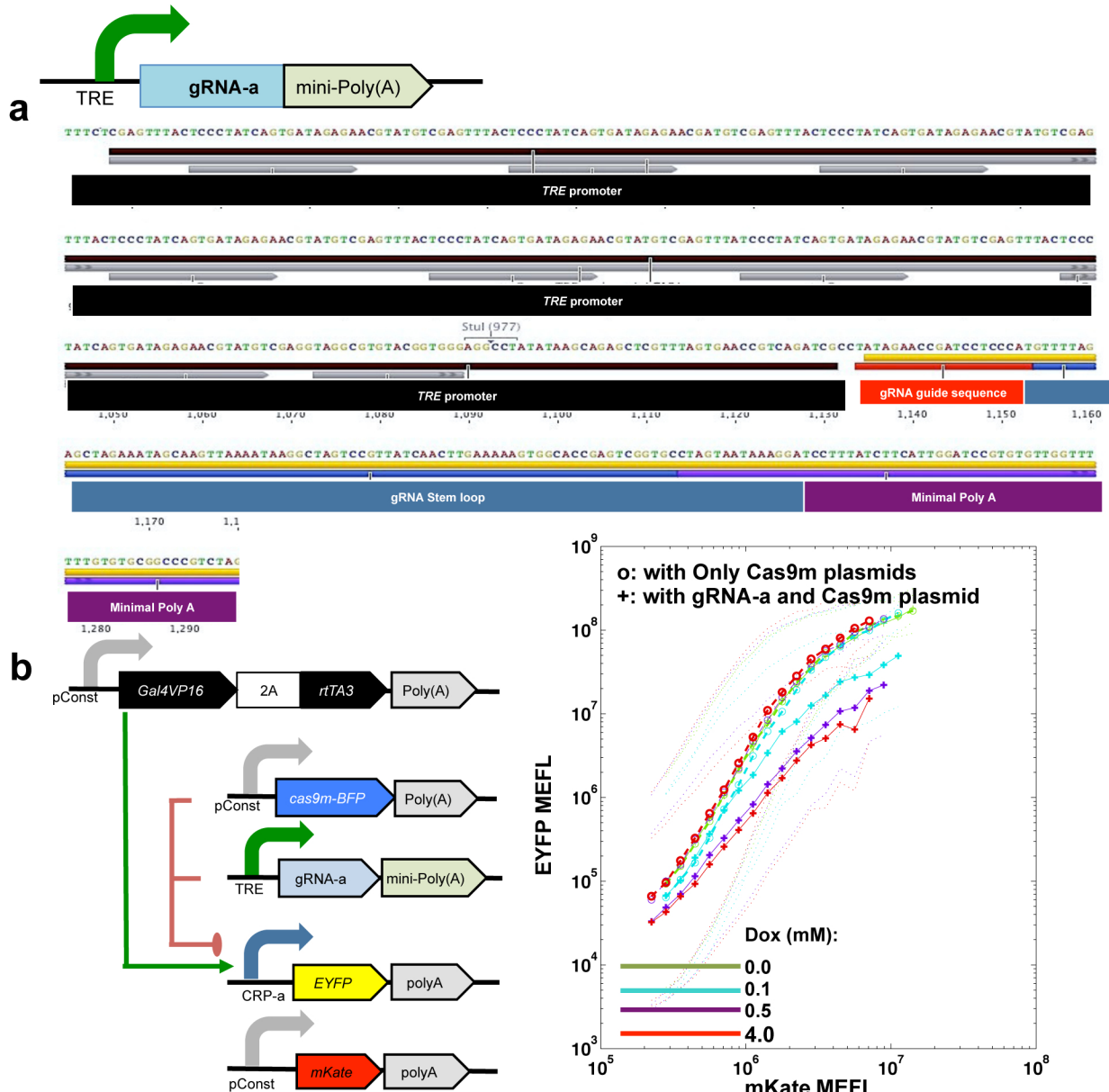
(a) A circuit containing a *U6/gRNA* repression device together with the gRNA target sites in *CRP-a* or *CRP-b*. **(b)** Comparison of output EYFP MEFL geometric mean when the promoter driving EYFP expression is either *CRP-b*, which should be targeted by gRNA-b, or *CRP-a* which should not be. Bars show geometric mean and standard deviation of EYFP MEFL means for cells expressing $\geq 10^6$ MEFL transfection marker mKate for gRNA-b and 3×10^6 for gRNA-a. $n=4$ biological replicates pooled from two representative experiments. **(c)** and **(d)** compare details of gRNA-b experiments to a negative control with no gRNA-b, showing output EYFP expression as a function of mKate constitutive fluorescence protein that serves as an indicator of relative circuit copy count. The repression of the matching promoter *CRP-b* is strong and increases with relative copy count, while the non-matching promoter (*CRP-a*) shows little effect from inclusion of gRNA-b, thus demonstrating minimal cross-talk from gRNA-b to *CRP-a*. Values shown are geometric mean (gRNA = black plus, no gRNA = red circle) and standard deviation (dotted lines) of EYFP expression subpopulations partitioned by constitutive fluorescence. Note that *CRP-b* data in panel b is also reported in Supplementary Fig. 3.

Supplementary Figure 5 Output EYFP as a function of constitutive fluorescent protein for *U6/CRa-U6/CRP-b* cascade.



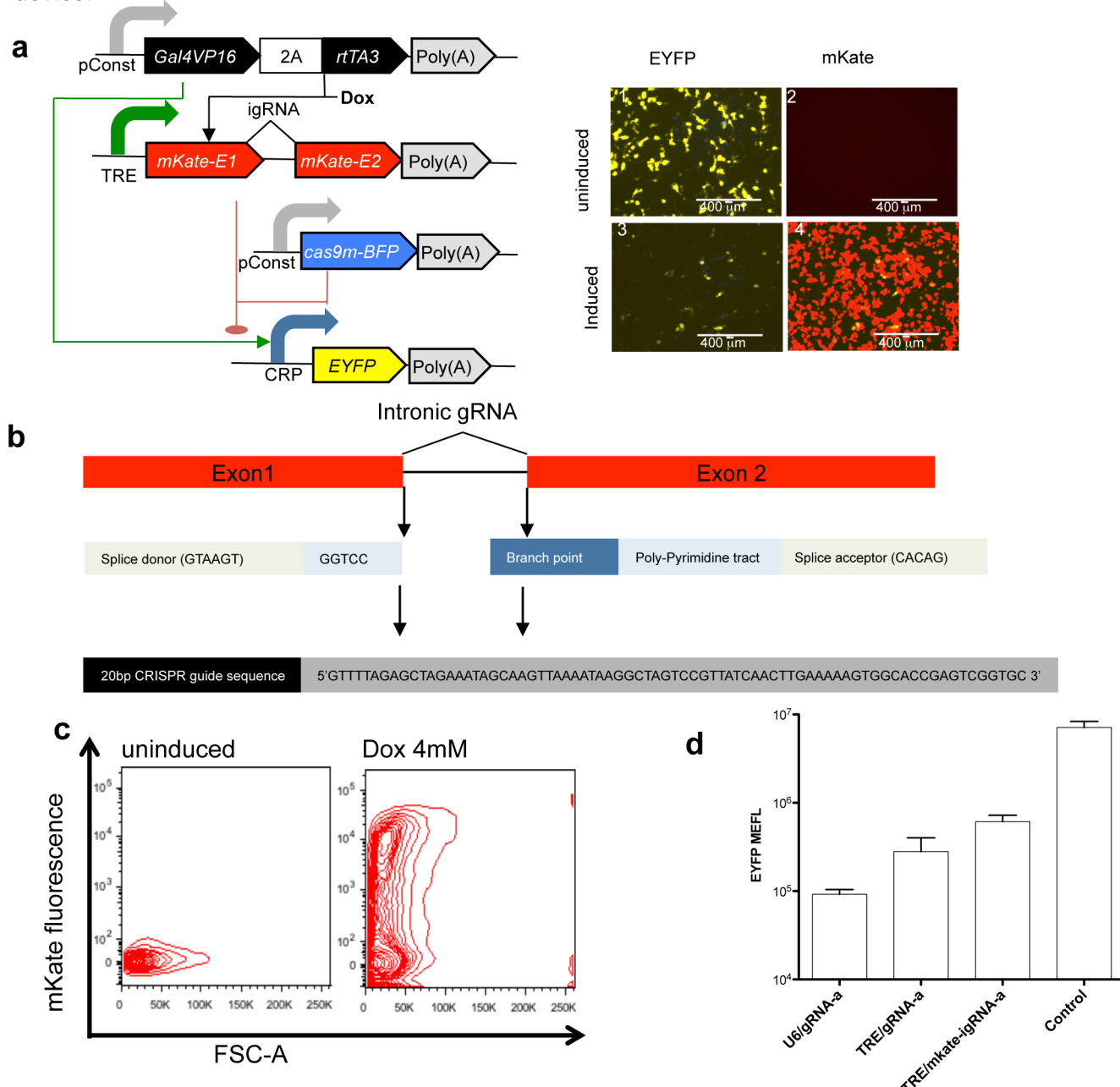
(a) EYFP MEFL as a function of plasmid copy count, indicated by constitutive fluorescence protein (mKate) MEFL, in the presence or absence of U6/gRNA-a (stage 1) variant 3 as depicted in Fig. 1d. The values on the x-axis (mKate MEFL) are indicative of relative number of plasmid copies present within each cell. Maximum de-repression of about 50 fold is observed for highest mKate MEFL. **(b)** Representative microscopy images depict EYFP output in the presence and absence of stage 1.

Supplementary Figure 6 Design and function of direct gRNA-a regulation by TRE promoter, an RNA Pol II promoter.



(a) Sequence of RNA Pol II mediated gRNA-a expression. The gRNA sequence downstream of *mini-CMV* promoter is in close proximity to transcription initiation site (within 6 nucleotides), followed by a minimal poly adenylation sequence. **(b)** Circuit with a repression device using this promoter. **(c)** Output EYFP, as a function of relative circuit copy count as indicated by constitutive fluorescence protein (mKate) MEFL, showing this repressor device (pluses) induced with Dox as compared to a negative control (circles) where the *TRE/gRNA-a* plasmid is replaced with an empty plasmid ($n=3$ biological replicates pooled from three representative experiments). The repressor device shows reduction of EYFP output with addition of Dox, while no effect is observed for the empty plasmid. Values shown are geometric mean and standard deviation (dotted lines) of EYFP expression in subpopulations partitioned by constitutive fluorescence.

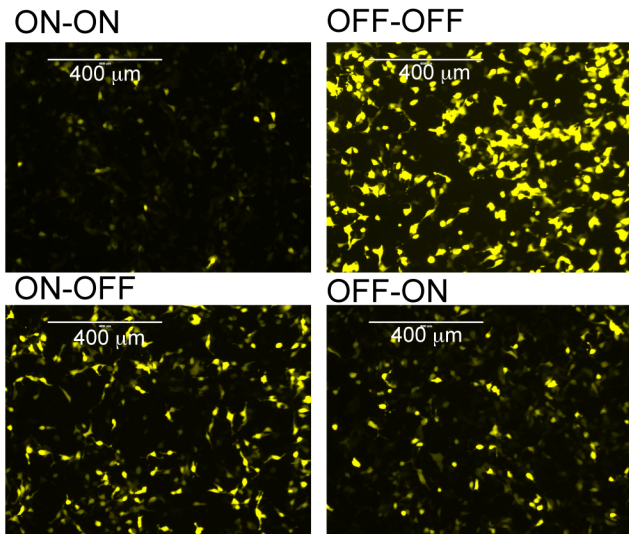
Supplementary figure 7 Design and function of intronic gRNA (igRNA) based repression device.



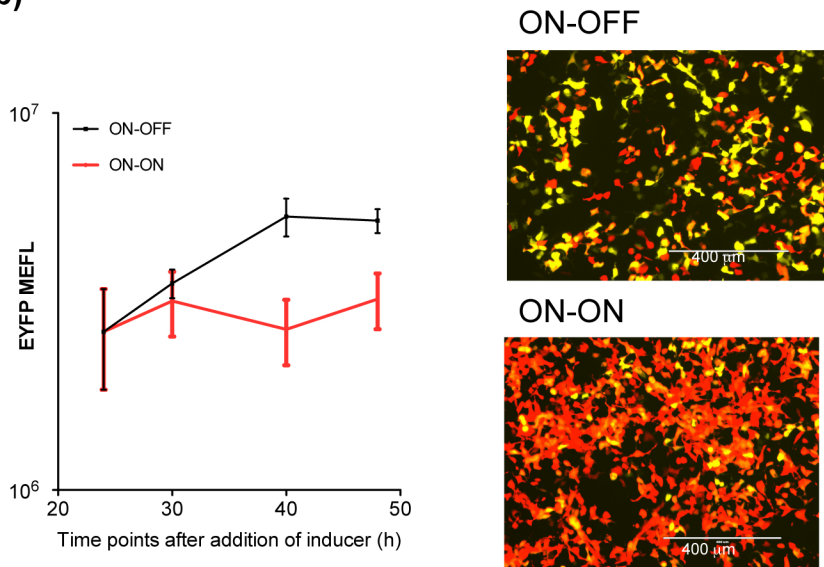
(a) Circuit with a repression device based on gRNA expressed from an intron inserted within mKate sequence. On the right, The four image panels include representative microscopy images for igRNA-a device in uninduced or fully induced by Dox conditions. Upon addition of Dox, mKate and igRNA-a are expressed (panel 4 versus panel 2) and this represses EYFP (panel 3) in comparison to uninduced condition (panel 1). **(b)** gRNA design as intron of mKate fluorescent protein coding gene. An artificial intron is created within mKate coding sequence using appropriate splicing sequences flanking the gRNA sequence. **(c)** Splicing of the intron is observed via mKate fluorescence by flow cytometry after induction of the device with Dox that drives mKate-igRNA expression from *TRE* promoter. **(d)** Side by side comparison of RNA Pol II driven gRNA-a devices presented throughout this study with standard *U6* driven gRNA-a device. All data have been reported in other figures. Bar graph represents geometric mean and standard deviation of EYFP MEFL means in samples transfected with all units of devices (gRNA and Cas9) for cells expressing $> 10^5$ MEFL of transfection unit, BFP. Control group corresponds to transfection with all the transcript units but not gRNAs.

Supplementary Figure 8 Investigating the reversibility of inducible CRISPR transcriptional repression devices.

(a)

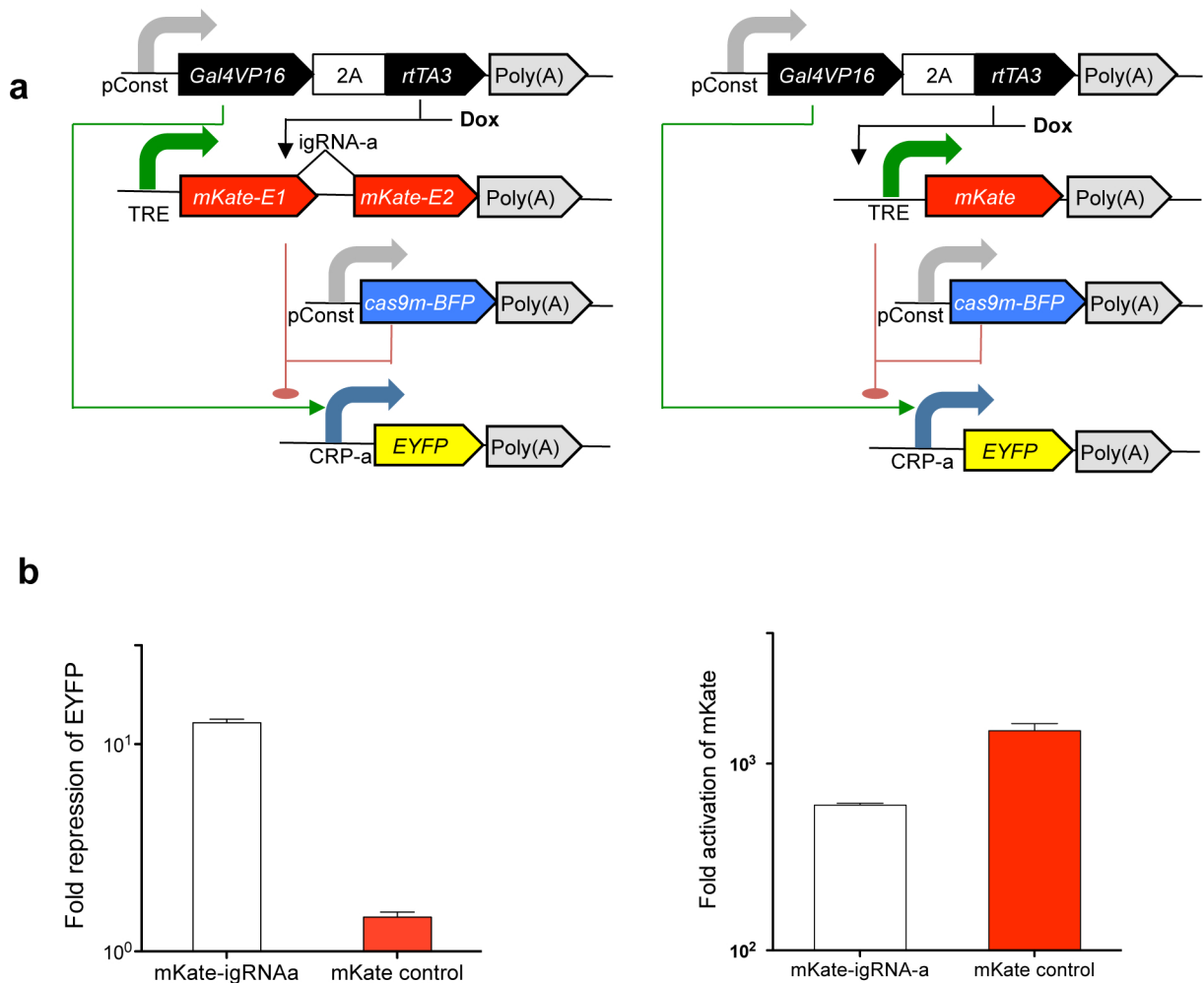


(b)



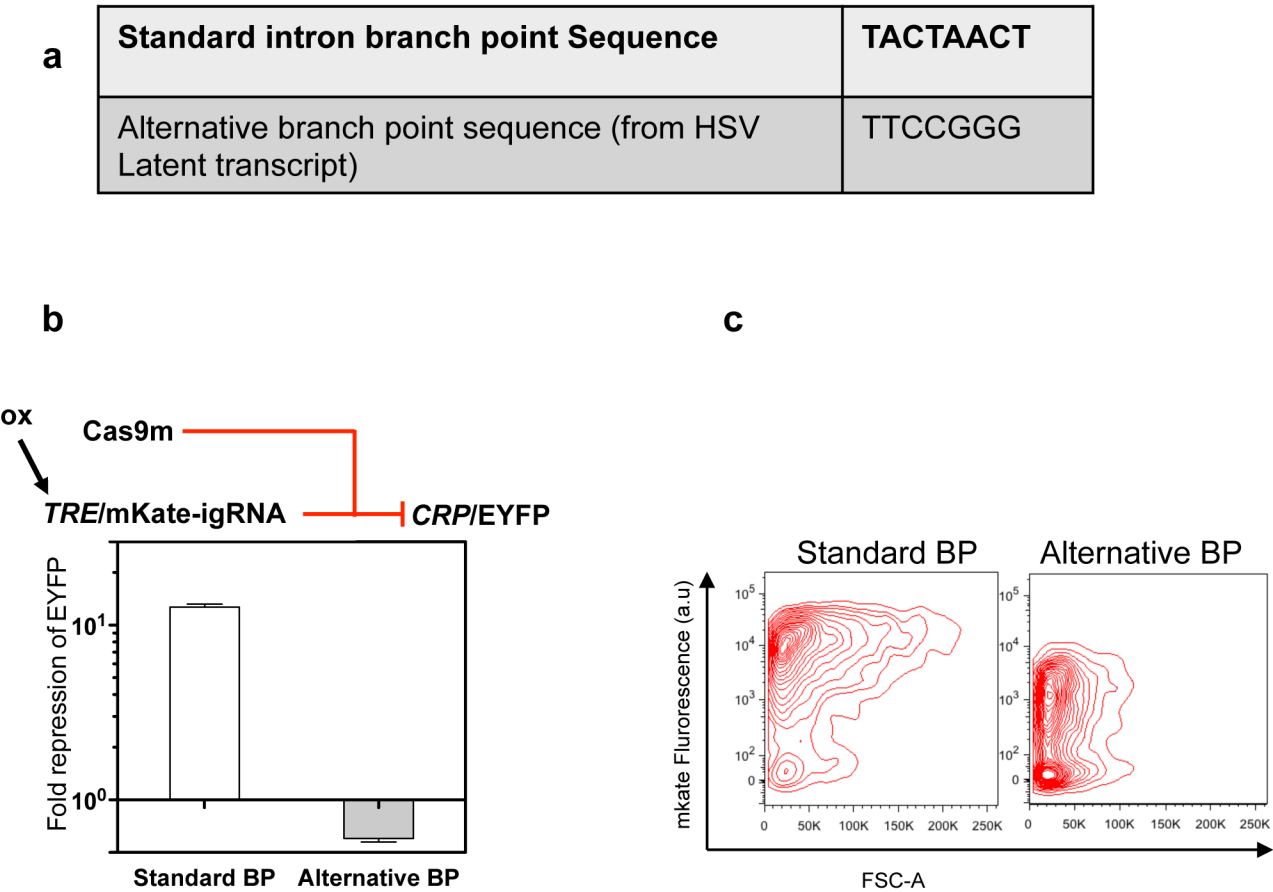
(a) Representative microscopy images of cells transfected with inducible igRNA-b device as shown in Fig. 2c bottom graph. Cells were induced with Dox for 12 hours and then divided into four groups according to whether they were continued under Dox induction (ON) or cultured without Dox (OFF). Images were captured 54 hours after Dox change. **(b)** Analysis of the reversibility of repression by an igRNA-a device: "ON" samples were induced with 4 mM Dox for 24 hours. Removal of Dox in this condition leads to increased EYFP levels. In the "ON-OFF" group, 24 hours after removal, the level of EYFP is about twice as high as in samples that were maintained in Dox for 48 hours. Data represent geometric mean and standard deviation of EYFP MEFL means for cells expressing $> 7 \times 10^7$ MEFL of transfection marker BFP. $n=3$ biological replicates from one representative experiments.

Supplementary Figure 9 Repression of output in the intronic gRNA device is not due to overexpression of mKate protein and load on host cellular resources.



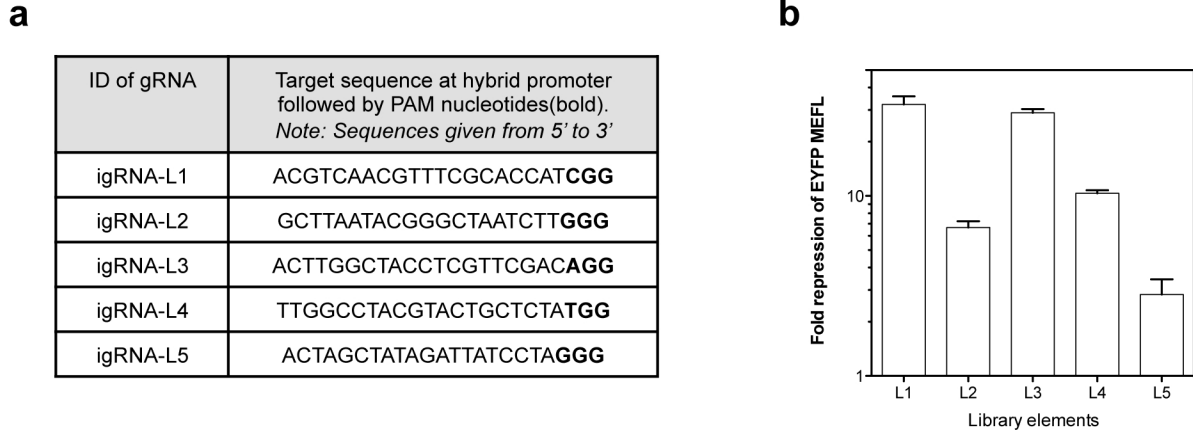
(a) Circuits with two devices, one including igRNA-a expressed as an intron of mKate fluorescence protein (left) and one containing only mKate fluorescence protein expressed under *TRE* (right). **(b)** Removal of igRNA-a reduces repression of the devices, suggesting that the observed behavior is not due to load on host cellular resources imposed by accompanying protein expression. Comparing uninduced and fully induced (4 mM Dox) conditions, EYFP expression decreases 12-fold with igRNA-a and only 1.5-fold with *TRE*/mKate, while mKate expression is induced approximately 1000-fold in both cases. Bars show geometric mean ratio and standard deviation of EYFP MEFL mean ratio for cells expressing $\geq 10^5$ MEFL constitutive Cas9m-BFP. $n=3$ biological replicates from one of two representative experiments for *TRE*/mKate data. Note that *TRE*/mKate-igRNA-a data is also reported in Fig. 2b and repeated here for comparison purposes.

Supplementary Figure 10 Cas9m and igRNA-a repression is reduced by modification of intronic branch point sequence.



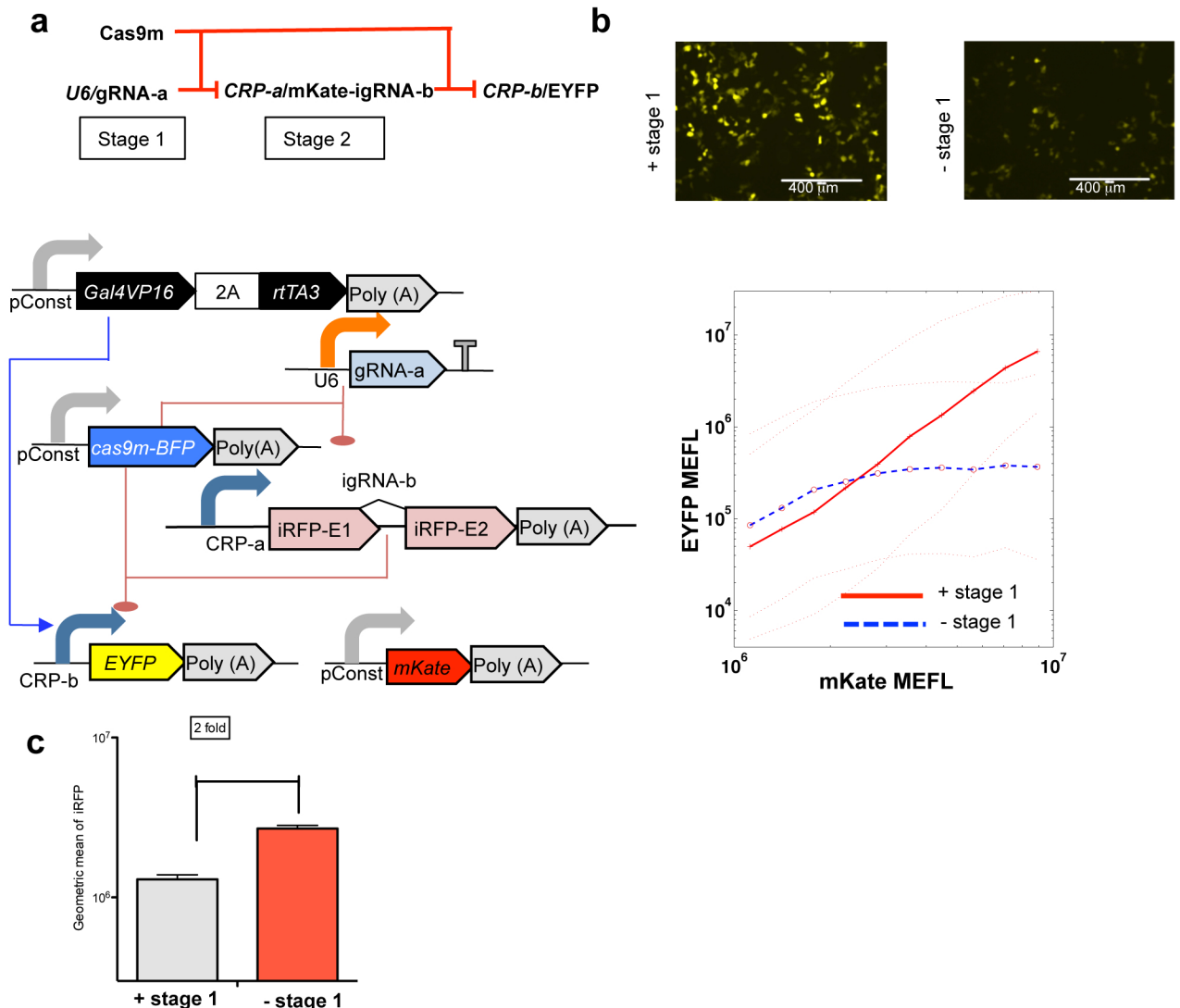
(a) Sequences for the widely used intronic branch point that contains the nucleotide A (adenosine) and a branch point sequence from HSV latent transcript that is resistant to de-branching and contains G (Guanosine). **(b)** Comparison of repression efficiency of devices for igRNA-a with standard branch point sequence (BP) or igRNA-a with alternative BP sequence. Bars show geometric mean ratio and standard deviation of EYFP MEFL mean ratio of fully induced (4 mM Dox) and uninduced conditions, for cells expressing $\geq 10^5$ MEFL of constitutive Cas9m-BFP. $n=3$ biological replicates pooled from three representative experiments. Note that standard BP data are also reported in Fig. 2b and Supplementary Fig. 8 and repeated here for comparison purposes. **(C)** mKate fluorescence in transfected population. Insertion of alternative branch point sequence decreases mKate expression compared to the standard BP sequence, but the expression levels are comparable.

Supplementary Figure 11 igRNA device library showing the nucleotide sequence of target sites at CRP promoters and corresponding guide sequence on igRNA.



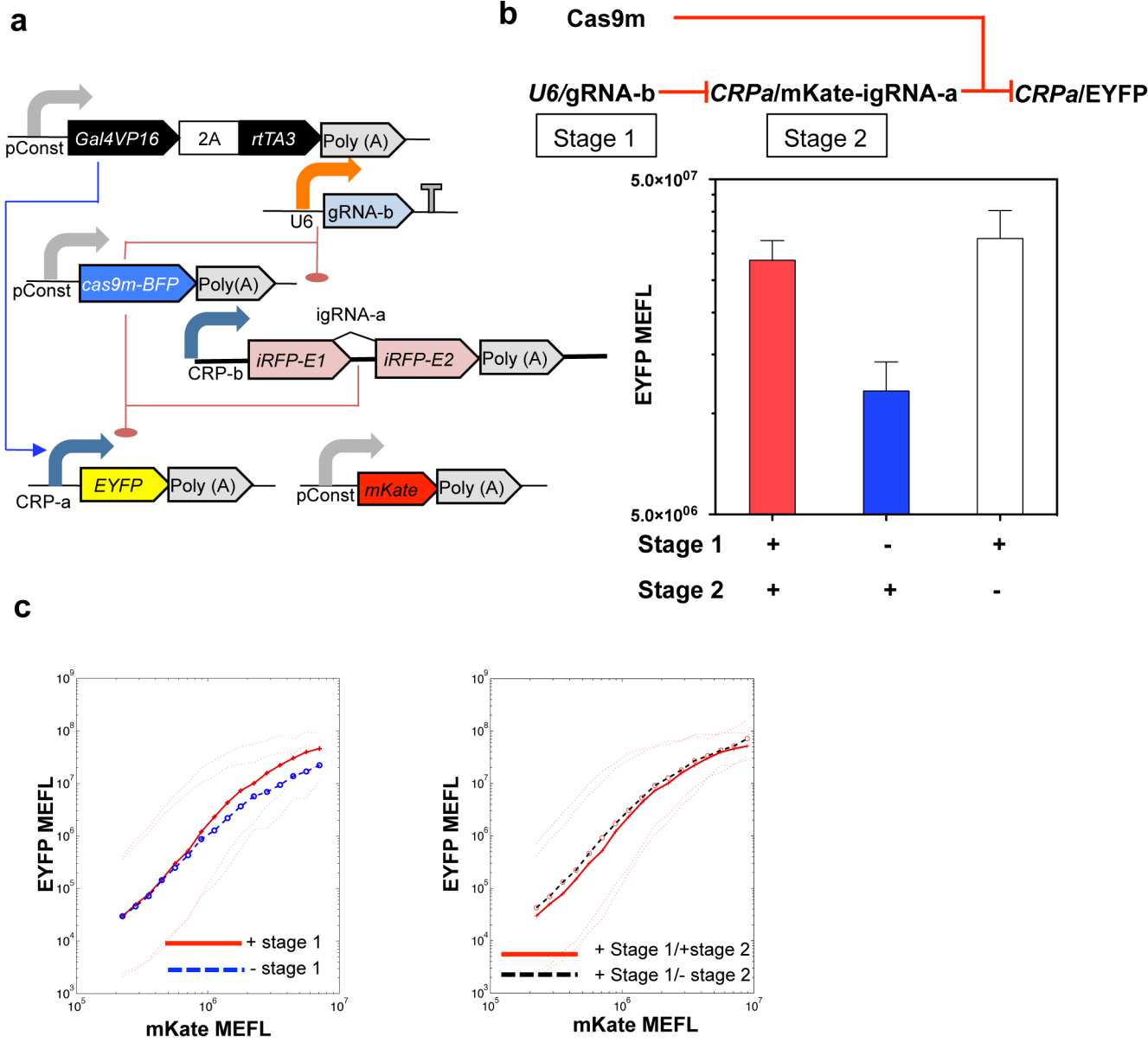
(a) Nucleotide sequence composition of the target site for each library member. The library sequences were rationally designed by modification of the gRNA-a target sequence based on current knowledge of CRISPR targeting specificity . Specifically, we inserted at least one or more mismatch within the first five nucleotides immediately upstream of PAM that has been shown to be essential for CRISPR specificity and a number of additional mismatches from nucleotide 5-20 upstream of this sequence, thereby aiming for orthogonality within the library. **(b)** Fold repression of EYFP (output) in the fully induced relative to uninduced conditions. By changing the sequence of the target site we can generate devices with a range of regulatory behavior. Bars show geometric mean ratio and standard deviation of mean ratio of EYFP MEFL in uninduced vs. fully induced samples, for cells expressing $\geq 10^7$ MEFL transfection marker. $n=3$ biological replicates pooled from two representative experiments. In our library, we did not detect any correlation between repression efficiency and AT content of target sequence nor the N nucleotide identity of NGG (PAM sequence) (data not shown), though such correlation may become apparent with larger libraries.

Supplementary Figure 12 Cascade circuit based on layering *U6* driven gRNA-a and *CRP* driven igRNA-b.



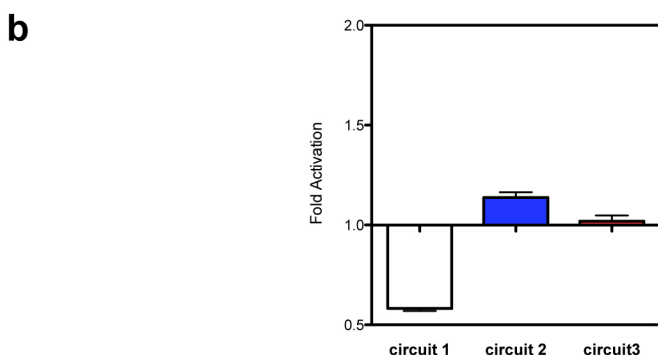
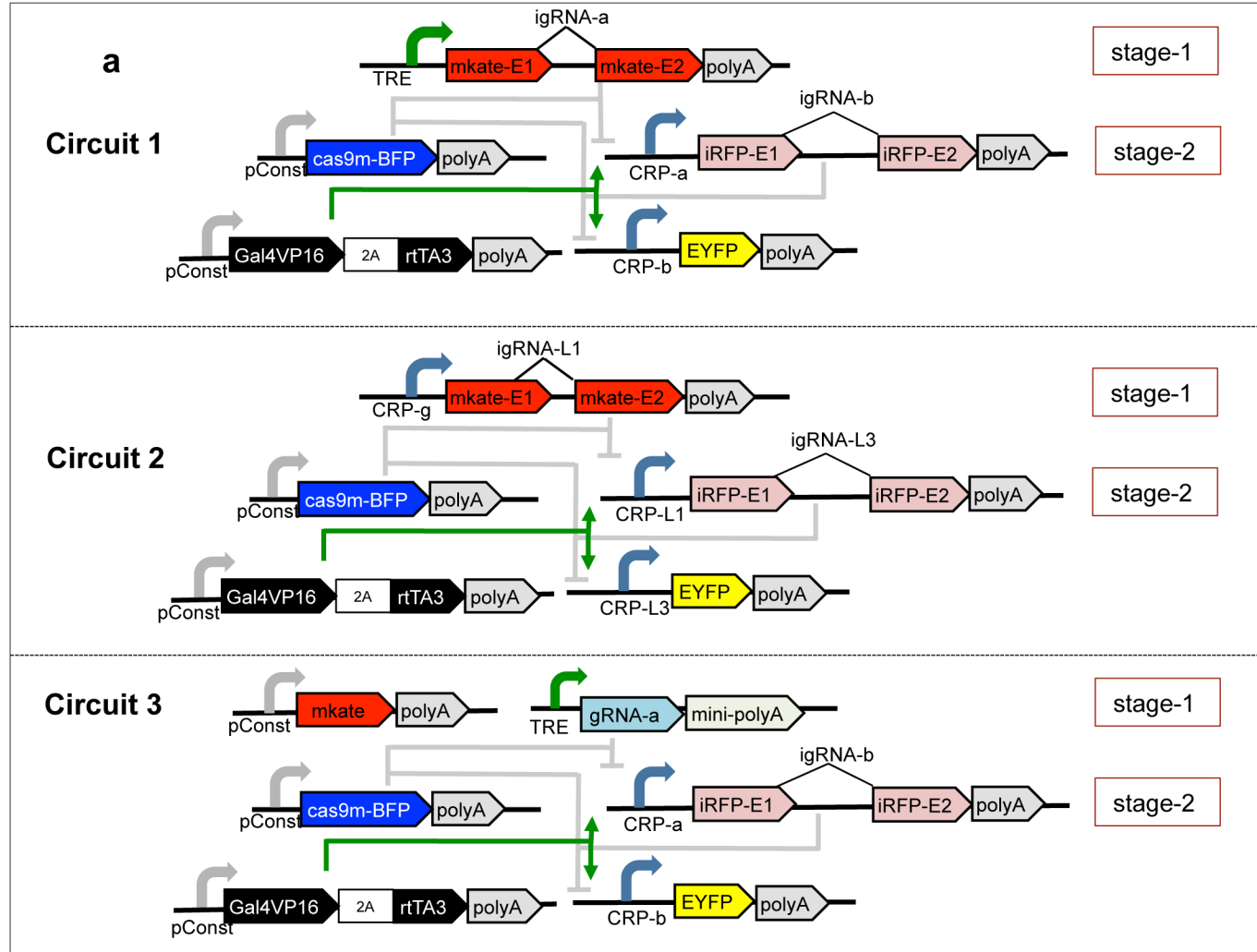
(a) A cascade of two transcriptional repressors with a *U6*/gRNA-a device connected to a *CRP*-a/igRNA-b device. Output EYFP and igRNA-b are both activated by binding of Gal4VP16 to its cognate sites at the *CRPs*. In the absence of stage 1 (*U6* driven gRNA-a), Cas9m is targeted to the *CRP*-b promoter by igRNA-b expressed from *CRP*-a as an intron in the iRFP coding sequence. As a result, Cas9m/igRNA-b represses EYFP expression from *CRP*-b promoter. In the presence of stage 1, Cas9m and gRNA-a mediated targeting to *CRP*-a promoter decreases igRNA-b expression, and this alleviates repression of EYFP. **(b)** Output (EYFP MEFL) as a function of relative circuit copy count, as indicated by constitutive fluorescence protein (mKate MEFL), in the presence or absence of *U6*/gRNA-a (stage 1). Maximum de-repression of approximately 20-fold is observed at the highest relative circuit copy count. Representative microscopy images illustrate EYFP fluorescence in the presence or absence of stage 1. **(c)** To confirm that the de-repression effect observed on CRISPR layered circuitry following inclusion of gRNA-a (stage 1) is not due to loss of function of CRISPR after introduction of two gRNAs, we analyzed iRFP level (stage 2 protein from which igRNA-b is expressed). Upon addition of stage 1 we observed about 2 fold repression in iRFP expression which confirms that stage 1 is repressing gRNA-b expression and is in fact layered. Data presented is geometric mean and standard deviation of iRFP mean for cells expressing $>3 \times 10^6$ MEFL. $n=4$ biological replicates pooled from two representative experiments.

Supplementary Figure 13 Cascade circuit based on layering *U6* driven gRNA-b and *CRP-b/igRNA-a*.



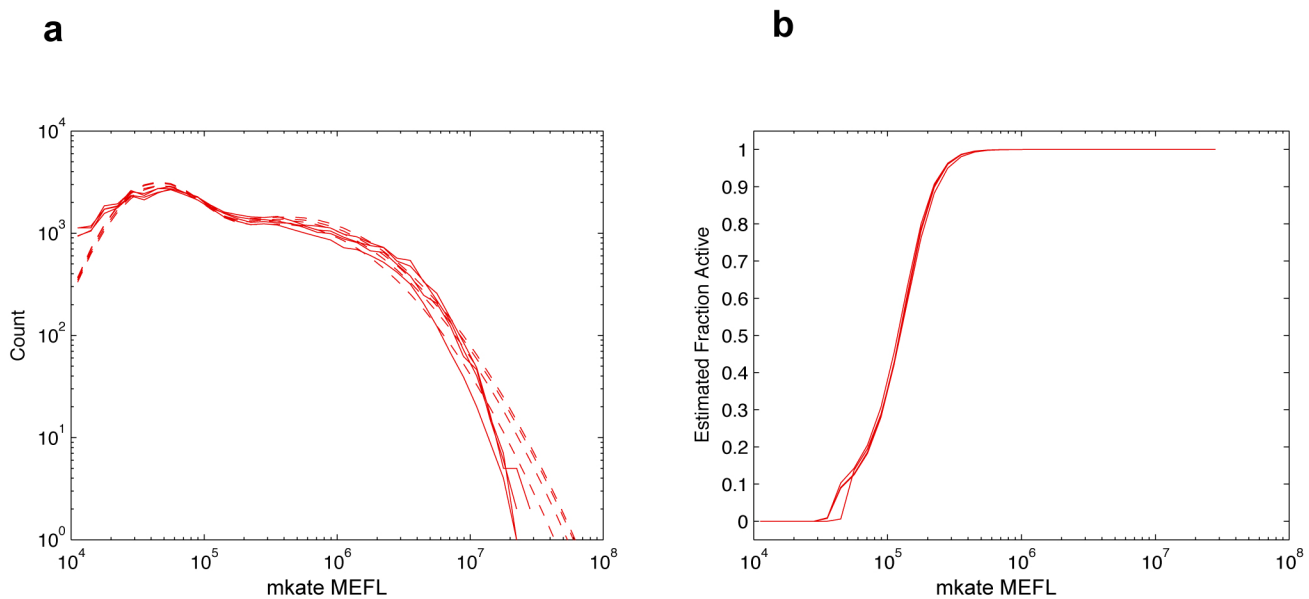
(a) A cascade of two transcriptional repression devices where *U6* promoter driven gRNA-b represses igRNA-a expression by binding the *CRP-b* promoter that drives expression of igRNA-a as an intron of iRFP, thus relieving EYFP repression caused by Cas9m and igRNA-a binding its promoter, *CRP-a*. **(b)** Output EYFP expression for the above cascade, with approximately 2.5 fold increase in EYFP level when stage 1 is added. In the absence of igRNA-a (stage 2), EYFP remains high, suggesting minimal direct interference between stage 1 and output *CRP-a* promoter. Bars show geometric mean and standard deviation of EYFP MEFL mean for cells expressing $\geq 10^6$ MEFL transfection marker mKate. $n=3$ biological replicates pooled from two representative experiments. **(c)** Details of EYFP as a function of relative circuit copy count, as indicated by constitutive mKate fluorescence, in the presence and absence of stage 1 (left panel) or in the presence and absence of stage 2 (right panel). Note that the impact of adding stage 1 increases at higher relative circuit copy count.

Supplementary Figure 14 Three cascades of transcriptional repression devices with stage 1 gRNAs expressed from RNA Pol II promoters.



(a) Three different cascades with transcriptional repression devices in which the gRNA of stage 1 is expressed from an RNA Pol II promoter, either as an intron (circuit 1 and 2) or directly (circuit 3). **(b)** Fold increase in output EYFP for these three cascades was measured. Bars show geometric mean ratio and standard deviation of EYFP MEFL mean ratio of fully induced gRNA-a vs. without igRNA-a, for cells expressing $\geq 10^5$ MEFL of constitutive Cas9m-BFP. $n=3$ biological replicates from one of two representative experiments. In this configuration and with parameters tested, none of the circuits exhibited significant activation.

Supplementary Figure 15 Typical distribution of constitutive fluorescence



Constitutive fluorescence (mKate) in transient co-transfection typically exhibits a bimodal lognormal distribution. **(a)** The distribution of constitutive fluorescence in a logarithmic histogram with 10 bins/decade for the negative control samples for gRNA-a in Fig. 1b (solid), and a bimodal lognormal model fit against each (dashed). **(b)** An estimate of the fraction of data from successfully transfected cells at any given level of mKate, computed from the bimodal model fit. These are used to set low mKate MEFL cutoffs, below which data is discarded.

Supplementary Discussion

Impact of CRISPR-based devices on host dynamics

The promoter sequences in the devices reported in this study were adapted from a previously reported study evaluating TALEs binding to their cognate target sites and modified to allow CRISPR recognition and targeting¹. Nucleotide BLAST of these sequences finds no exact matches in the human genome². CRISPR specificity and off-target effects remain active areas of research³⁻⁸. The specificity of Cas9 is sequence- and locus-dependent and appears to be governed by the quantity, position and identity of mismatching bases. While prior reports have suggested that 8-12 nucleotides proximal of PAM is essential for specificity⁵, another recent report demonstrates that specificity is defined by exact matching of the PAM-proximal 5 bp to the guide sequence⁴. Studies such as ours, and the generation and characterization of larger libraries of engineered regulatory devices will further improve the understanding of CRISPR specificity.

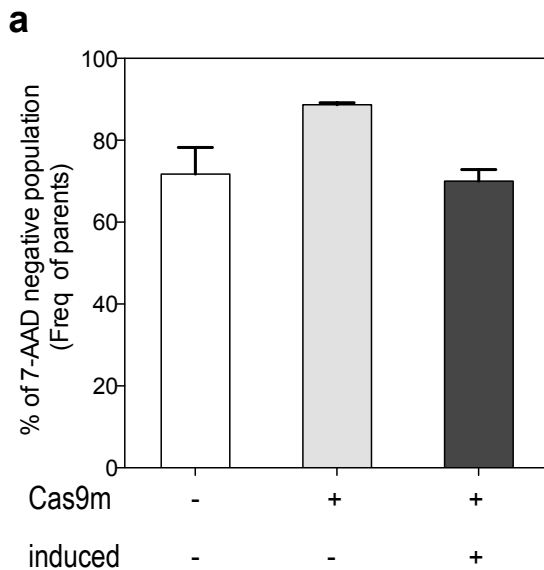
In our study we used a catalytically mutant Cas9 not fused to any effector domain. We believe that the absence of an effector domain reduces deleterious effects in potential off-target binding sites. In addition, in our study we kept the level of transfected Cas9m as low as possible, transfecting 2×10^5 HEK293 cells with only 70ng of Cas9m, which has been suggested to decrease off-target effects.³ Although the efficacy of these strategies is still unclear, they may contribute to the low toxicity observed in our study: flow cytometry analysis of cell viability using 7-Aminoactinomycin-D (7-AAD) dye in the igRNA-a device revealed comparable viability across different conditions (**Supplementary Fig. A.a**). This was also the case for the igRNA-b device (data not shown). Likewise, microscope observation of transfected cells did not show toxicity beyond levels expected following transfection of the cells (**Supplementary Fig. A.b**).

Additional Intronic gRNA Device Characterization

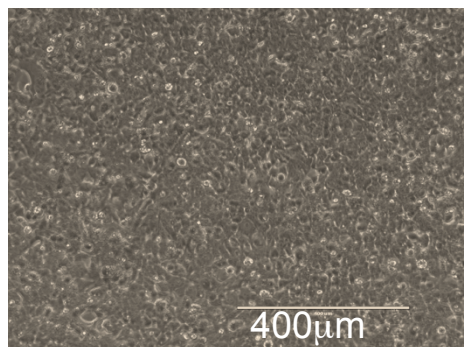
We assayed the intronic gRNA (igRNA) devices further. We inserted two stop codons within the intron sequence, which allowed us to verify proper splicing of intron by observing mKate fluorescence (**Supplementary Fig. 7**). To verify that the observed repression of the output is not due to co-expression of the input protein and load on host cellular resources, we removed the igRNA sequence and expressed comparable amount of mKate fluorescent protein. We did not observe significant repression of output in that configuration (**Supplementary Fig. 9**). To examine whether proper processing of spliced intron is required for the function of Cas9m/igRNA complex, we replaced the eukaryotic intron branch point sequence with a sequence from HSV latency-associated transcript, which interferes with proper de-branching of a spliced intron⁹. This modification resulted in diminished igRNA/Cas9m mediated repression efficiency (**Supplementary Fig. 10**), suggesting that Cas9m-mediated targeting requires efficient processing of the spliced igRNA.

1. F. Zhang, L. Cong, S. Lodato et al., *Nature biotechnology* **29** (2), 149 (2011).
2. S. F. Altschul, T. L. Madden, A. A. Schaffer et al., *Nucleic acids research* **25** (17), 3389 (1997).
3. Y. Fu, J. A. Foden, C. Khayter et al., *Nature biotechnology* **31** (9), 822 (2013).
4. X. Wu, D. A. Scott, A. J. Kriz et al., *Nature biotechnology* (2014).
5. P. D. Hsu, D. A. Scott, J. A. Weinstein et al., *Nature biotechnology* **31** (9), 827 (2013).
6. S. W. Cho, S. Kim, Y. Kim et al., *Genome research* **24** (1), 132 (2014).
7. P. Mali, J. Aach, P. B. Stranges et al., *Nature biotechnology* **31** (9), 833 (2013).
8. D. Carroll, *Nature biotechnology* **31** (9), 807 (2013).
9. J. M. Zabolotny, C. Krummenacher, and N. W. Fraser, *Journal of virology* **71** (6), 4199 (1997).

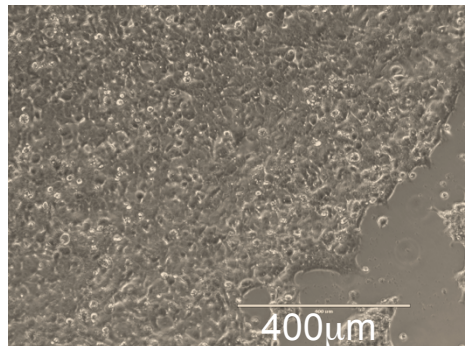
Figure A 7-AAD viability test following transfection with the igRNA-a device.



b Uninduced- With Cas9



Induced



(a) 7-Aminoactinomycin D (7-AAD) is a red-fluorescent dye with strong affinity towards dsDNA. Live cells are generally impermeable to this dye, allowing differentiation of live and dead cells by flow cytometry analysis of 7-AAD negative and positive populations respectively. 7-AAD has a maximum absorption at 545nm and a maximum emission at 650nm, allowing simultaneous measurement with other fluorescent proteins in our devices. As depicted in the bar graphs, the viability of cells was not significantly influenced by the presence of cas9m, igRNA-a or doxycycline. Bar graphs represent geometric mean and standard deviation of percentage of 7-AAD negative population ($n=3$ biological replicates from one of two representative experiments). **(b)** Bright-field images of cells in the uninduced (top) and induced (bottom) conditions does not indicate visible toxicity within the culture.

Supplementary notes:	Sequences used or made in this study
U6-gRNA-a	AAGGTGGGCAGGAAGAGGGCCTATTTCCCATGATTCTTCATATT TGCATATACGATAACAAGGCTTAGAGAGATAATTAGAATTAATTG ACTGTAACACAAAGATATTAGTACAAAATACGTGACGTAGAAAGT ATAAATTCTGGTAGTTGCAGTTAAAATTATGTTAAAATGG ACTATCATATGCTTACCGTAACCTGAAAGTATTGATTCTGGCT TTATATATCTTGAAAGGACGAAACACCG TATAGAACCGATCCT CCCATTTAGAGCTAGAAATAGCAAGTAAATAAGGCTAGTCC GTTATCAACTGAAAAAGTGGCACCGAGTCGGTCTTTTTT
U6-gRNA-b	AAGGTGGGCAGGAAGAGGGCCTATTTCCCATGATTCTTCATATT TGCATATACGATAACAAGGCTTAGAGAGATAATTAGAATTAATTG ACTGTAACACAAAGATATTAGTACAAAATACGTGACGTAGAAAGT ATAAATTCTGGTAGTTGCAGTTAAAATTATGTTAAAATGG ACTATCATATGCTTACCGTAACCTGAAAGTATTGATTCTGGCT TTATATATCTTGAAAGGACGAAACACCG TACCTCATCAGGAAC ATGTGTTAAGAGCTATGCTGAAACAGCAGAAATAGCAAGTTAA ATAAGGCTAGTCGTTATCAACTGAAAAAGTGGCACCGAGTCGGT GCTTTTTT
CRa-U6/gRNA-b (Version 1)	GGTTTACCGAGCTTATTGGTTTCAAACCTCATTGACTGTGCCA GGTCGGGCAGGAAGAGGGCCTATTCATGATTCTTCATATTG CATATACGATAACAAGGCTTAGAGAGATAATTAGAATTAATTGAC TGAAACACAAAGATATTAGTACAAAATACGTGACGTAGAAAGTAAT AATTCTGGTAGTTGCAGTTAAAATTATGTTAAAATGGACT ATCATATGCTTACCGTAACCTGAAATATAGAACCGATCCTCCATTG GTATATATCCAATGGGAGGATCGGTTCTACTTGTTGAAAGGACG AAACACCGTACCTCATCAGGAACATGTGTTAAGAGCTATGCTGGA AACAGCAGAAATAGCAAGTTAAATAAGGCTAGTCGTTATCAACT TGAAAAGTGGCACCGAGTCGGTCTTTTTGGTGCCTTTATG CTTGAGTATTGATAATGTTTT
CRa-U6/gRNA-b(version 2)	AAGGTGGGCAGGAAGAGGGCCTATTTCCCATGATTCTTCATATT TGCATATACGATAACAAGGCTTAGAGAGATAATTAGAATTAATTG ACTGTAACACAAAGATATTAGTACAAAATACGTGACGTAGAAAGT ATAAATTCTGGTAGTTGCAGTTAAAATTATGTTAAAATGG ACTATCATATGCTTACCGTAACCTGAAACCAATGGGAGGATCGGTT CTATATATATTAGAACCGATCCTCCATTGGCTTGTTGAAAG GACGAAACACCG TACCTCATCAGGAACATGTGTTAAGAGCTATG CTGAAACAGCAGAAATAGCAAGTTAAATAAGGCTAGTCGTTATCAAC CAACTGAAAAGTGGCACCGAGTCGGTCTTTTTGGTGCCTTTATG GCTTGAGTATTGATAATGTTTT
CRa-U6/gRNA-b(version 3)	GGTTTACCGAGCTTATTGGTTTCAAACCTCATTGACTGTGCCA GGTCGGGCAGGAAGAGGGCCTATTCATGATTCTTCATATTG CATATACGATAACAAGGCTTAGAGAGATAATTAGAATTAATTGAC TGAAACACAAAGATATTAGTACAAAATACGTGACGTAGAAAGTAAT AATTCTGGTAGTTGCAGTTAAAATTATGTTAAAATGGACT ATCATATGCTTACCGTAACCTGAAATATAGAACCGATCCTCCATTG GTATATATATTAGAACCGATCCTCCATTGGCTTGTTGAAAGGACG AAACACCG TACCTCATCAGGAACATGTGTTAAGAGCTATGCTG AAACAGCAGAAATAGCAAGTTAAATAAGGCTAGTCGTTATCAAC TGAAAAGTGGCACCGAGTCGGTCTTTTTGGTGCCTTTATG GCTTGAGTATTGATAATGTTTT
mKate-Intronic gRNA-b	TCTAAGGGCGAAGAGCTGATTAGGAGAACATGCACATGAAGCTG TACATGGAGGGCACCGTGAACAACACCACCTCAAGTGCACATCC GAGGGCGAAGGCAAGGCTACGAGGGCACCCAGACCATGAGAAAT CAAGGTGGTCGAGGGCGCCCTCTCCCCCTCGCCTGCACATCCT GGCTACCAGCTCATGTACGGCAGCAAACCTCATCAACCCACACC CAGGGCATCCCCGACTTCTTAAGCAGTCCTCCCTGAG GTAAAGT GGTCCTACCTCATCAGGAACATGTGTTTAGAGCTAGAAATAGCA AGTTAAAATAAGGCTAGTCGTTATCAACTGAAAAGTGGCACC GAGTCGGTCTACTCAACTCTGAGTCCTTTTTTACAGG GCTTCACATGGGAGAGTCACCATAGCAAGACGGGGCGTG CTGACCGCTACCCAGGACACCAGCCTCCAGGACGGCTGCCTCATC TACAACGTCAAGATCAGAGGGGTGAACTCCCACCAACGGCCCT GTGATGCAGAAGAAAACACTCGGCTGGAGGCCTCACCAGAGATG CTGTACCCCGCTGACGGCGGCTGGAAGGGCAGAAGCGACATGGC CCTGAAGCTCGTGGCGGGGCCACCTGATCTGCAACTTGAAGAC CACATACAGATCCAAGAAACCCGCTAAGAACCTCAAGATGCCGG CGTCTACTATGTGACAGAAGACTGGAAGAATCAAGGAGGCCGA CAAAGAGACCTACGTGAGCAGCACGAGGTGGCTGGCCAGATA CTGCG
mKate intronic gRNA-a	ATGGTGTCTAAGGGCGAAGAGCTGATTAGGAGAACATGCACATG

	AAGCTGTACATGGAGGGCACCGTGAACAACCACCACTTCAGTGC ACATCCGAGGGCGAAGGCAAGCCCTACGAGGGCACCCAGACCAT GAGAATCAAGGTGGTCGAGGGCGGCCCTCTCCCTCGCCTTCGA CATCCTGGCTACCAGCTTCATGTACGGCAGCAAACCTTCATCAAC CACACCCAGGGCATCCCGACTTCTTAAGCAGTCCTCCCTGAG GTAAGTGGTCTATAAGAACCGATCCTCCATTTAGAGCTAGA AATAGCAAGTAAATAAGGCTAGTCGTTATCAACTTGAAAAG TGGCACCGAGTCGGTCTACTAACTCGAGTCCTTTTTTC ACAGGGCTTCACATGGGAGAGAGTACCCACATACGAAGACGGGG GCGTGTGACCGCTACCCAGACACCAGCCTCCAGGACGGCTGC CTCATCTACACGTCAGATCAGAGGGTGAACCTCCCATTCCAACG GCCCTGTGATGAGAAGAAAACACTCGGCTGGAGGCCCTCACC GAGATGCTGTACCCCGTGCAGGGCGCTGGAGGCAGAAGCGA CATGGCCCTGAAGCTCGTGGCGGGGCCACCTGATCTGAACCT GAAGACCACATACAGATCCAAGAAACCCGCTAAGAACCTCAAGAT GCCCGCGTCTACTATGTGGACAGAAGACTGGAAAGAATCAAGGA GGCCGACAAGAGACCTACGTCGAGCAGCAGCAGGTTGGCTGG CCAGATACTGCGACCTCCCTAGCAAACCTGGGCACAAACTTAATTG A
CRP α promoter	GCTCCGAATTCTCGACAGATCTCATGTGATTACGCCAAGCTACGG GCGGAGTACTGTCCTCCGAGCGGAGTACTGTCCTCCGAGCGGAG TACTGTCCTCCGAGCGGAGTACTGTCCTCCGAGCGGAGTCTGTC CTCCGAGCGGAGACTCTAGATATAGAACCGATCTCCATTGGAAT TCTAGGCCTGTACGGTGGAGGCCTATATAAGCAGAGCTCGTTA GTGAACCGTCAGATCGCCTCGAGTATAGAACCGATCTCCATTG GATCCAATTGAC
CRP β promoter	GCTCCGAATTCTCGACAGATCTCATGTGATTACGCCAAGCTACGG GCGGAGTACTGTCCTCCGAGCGGAGTACTGTCCTCCGAGCGGAG TACTGTCCTCCGAGCGGAGTACTGTCCTCCGAGCGGAGTCTGTC CTCCGAGCGGAGACTCTAGATACCTCATCGGAACATGTTGGATT CTAGGCCTGTACGGTGGAGGCCTATATAAGCAGAGCTCGTTAG TGAACCGTCAGATCGCCTCGAGTACCTCATCGGAACATGTTGGAT CCAATTGAC
iRFP-igRNA-a	ATGGCTGAAGGATCCGTGCCAGGCAGGCTGACCTTGTACCTGC GACGATGAGCCGATCCATATCCCCGGTGCCTACCAACCGCATGGA CTGCTGCTCGCCCTCGCCGCGACATGACGATCGTTGCCGGCAG CGACAAACCTCCCGAACTCACCGGACTGGCGATCGGCCGCGCTGAT CGGCCGCTCTGGCCGGATGCTTCGACTCGGAGACGCCAACACC GTCTGACGATCGCCTTGGCCGAGCCCCGGGGCGCCGTCGGAGCA CCGATCACTGTCGGCTTACCGATGCGAAAGGTAGTGGTCTATA GAACCGATCCTCCATTTAGAGCTAGAAATAGCAAGTAAAG TAAGGCTAGTCGTTATCAACTTGAAAAGTGGCACCGAGTCGG TGCTACTAATCTCGAGTCCTTTTTTACAGGACGCAGG CTTCATCGCTCTGGCATGCCATGATCAGCTCATCTCTCGAG CTCGAGCCTCCCAAGCGGGGACGTCGCCAGGCCAGGGCTT CCGCCGACCAACAGGCCATCCGCCCGCTGCAGGCCGCGAAA CCTTGGAAAGGCCCTGCGCCGCCGCGCAAGAGGTGCGGAAG ATTACCGGCTCGATGGGTGATGATCTATGCTTCGCTCCGACT TCAGCGCGAAGTGTGATCGCAGAGGATCGGTGCGCCGAGGTGAG TCAAAACTAGGCCTGCACTATCTGCCTAACCGTGCCTGGCGAG GCCCGTCGGCTTACCATCAACCGGTACGGATCATTCCGAT ATCAATTATCGGCCGGTGCCTGGTACCCAGACCTCAATCCGGTC ACCGGGCGGCCGATTGATCTTAGCTTCGCCATCTGCGCAGCGTC TCGCCCGTCCATGGAAATTATGCGCAACATAGGCATGCAAGGC ACGATTCGATCTGATTTGCGCGGGAGCGACTGTGGGATTG ATCGTTGCCATACCGAACGCCGTACTACGTCGATCTGATGGC GCCCAAGCCTGCGAGCTAGTCGCCAGGTTCTGGCCTGGCAGAT CGCGTGTGGAGAGTGA
iRFP-igRNA-b	ATGGCTGAAGGATCCGTGCCAGGCAGGCTGACCTTGTACCTGC GACGATGAGCCGATCCATATCCCCGGTGCCTACCAACCGCATGGA CTGCTGCTCGCCCTCGCCGCGACATGACGATCGTTGCCGGCAG CGACAAACCTCCCGAACTCACCGGACTGGCGATCGGCCGCGCTGAT CGGCCGCTCTGGCCGAGCCCCGGGGCGCCGTCGGAGCA CCGATCACTGTCGGCTTACCGATGCGAAAGGTAGTGGTCTACC TCATCAGGAACATGTGTTAGAGCTAGAAATAGCAAGTAAAG AAGGCTAGTCGTTATCAACTTGAAAAGTGGCACCGAGTCGG GCTACTAATCTCGAGTCCTTTTTTACAGGACGCAGG TTCATCGCTCTGGCATGCCATGATCAGCTCATCTCCTCGAGC

	TCGAGCCTCCCCAGCGGGACGTGCGCGAGCCGCAGGCCTTCTTC CGCCGCACCAACAGCGCCATCCGCCGCTGCAGGCCGCCAAC CTTGGAAAGCGCCTGCGCCGCCGCCGCAAGAGGTGCGGAAGA TTACCGGCTTCGATCGGGTGATGATCTATCGCTTCGCCCTCGACTT CAGCGCGAAGTGATCGCAGAGGATCGGTGCGCCGAGGTCGAGT CAAAACTAGGCCTGCACTATCCTGCCCTAACCGTGCCGGCGCAGG CCCGTCGGCTCTATACCATCAACCCGGTACGGATCATTCCGATAT CAATTATCGGCCGGTGCGGTACCCCCAGACCTCAATCCGGTCAC CGGGCGGCCGATTGATCTTAGCTTCGCCATCCGCGCAGCGTCTC GCCCGTCCATCTGGAATTCATGCGAACATAGGCATGCACGGCAC GATGTCGATCTGATTTGCCGGGGAGCGACTGTGGGATTGAT CGTTGCCATCACCGAACGCCGTACTACGTCGATCTGATGCCG CCAAGCCTGCGAGCTAGTCGCCAGGTTCTGGCCTGGCAGATCG GCGTGATGGAAGAGTGA
--	---